Green Synthesis of rGO-AgNP Composite Using *Curcubita Maxima* Extract for Enhanced Photocatalytic Degradation of the Organophosphate Pesticide Chlorpyrifos

Karthik Chinnappa (karthikc@stjosephs.ac.in)
St. Joseph's College of Engineering https://orcid.org/0000-0002-3912-0371
Punnaivalavan Karuna Ananthai
St. Joseph's College of Engineering
Pandi Prabha Srinivasan
Sri Venkateswara College of Engineering
Caroline Dharmaraj Glory Bai
St. Joseph's College of Engineering

Research Article

Keywords: One-pot green synthesis, adsorption, nanocomposite, photocatalytic activity, wastewater treatment

Posted Date: January 28th, 2022

DOI: https://doi.org/10.21203/rs.3.rs-1243946/v1

Version of Record: A version of this preprint was published at Environmental Science and Pollution Research on April 1st, 2022. See the published version at https://doi.org/10.1007/s11356-022-19917-1.

Abstract

Chlorpyrifos is a broad-spectrum organophosphate pesticide widely used for agricultural and non-agricultural applications that can highly intervene and impact with the ecosystem and affects both biotic and abiotic components. Photocatalytic degradation process using nanoparticles and nanocomposites are more fascinating as they are rapid and efficient than the existing other degradation routes. In this study, *Curcubita maxima* leaves are used as a novel source for green synthesis of reduced graphene oxide - silver composite in a single pot. Characterization of the novel phyto source driven composite was performed by UV-visible spectroscopy, Fourier transform infrared analysis, X-ray diffraction analysis and field emission scanning electron microscopic methods. The assessment of degradation effect of chlorpyrifos by the synthesized nanocomposite was performed. The photocatalytic activity of the composite was demonstrated through two different process as adsorption under room temperature and photocatalysis in the presence of sunlight. Different parameters such as pH, time, photocatalyst dose and pesticide concentration were optimized. The adsorption isotherms governing the photocatalytic adsorption process were investigated to predict the adsorption capacity of the synthesized nanocomposite. In addition, the results of antimicrobial activity of the nanocomposite against gram-positive, gram-negative bacteria and antifungal activity were also been found to be highly promising to utilize this composite for the removal of microbial contaminations in wastewater treatment.

Introduction

Chlorpyrifos [O, O-diethyl O-(3, 5, 6-trichlor-2-pyridyl) phosphorothioate] (CP) is a broad spectrum organophosphate (OP) pesticide widely used for agricultural and non-agricultural applications. This pesticide can highly intervene and affect the ecosystem and effect up to the radius of 24 km around the site of application (Das et al. 2017). The extensive usage of CP resulted in its persistence into the environment (soil, ground water, and air), agricultural products and its byproducts. Such bioaccumulation of the CP into the food web ecosystem affects both biotic and abiotic components. Cardiovascular disorders, central nervous system related disorder due to acetylcholine esterase inhibition, respiratory tract issues are some of the effects of CP bioaccumulation to humans and notorious impact on fishes are also identified as some of the health issues related to CP (Bootharaju and Pradeep 2012; Yang et al. 2008; Deb and Das 2013). Apart from being immunotoxin and neurotoxin to humans, CP also adversely affects the microbiota population such as bacteria, fungi, algae of the soil as well as impression with the mineralization process and nitrogen fixation (Akbar and Sultan 2016). Therefore, the concern for addressing the global ecosystem threat due to high accumulation of CP, gains more interest on research avenues.

The need for appropriate green remediation techniques has driven application of microbial enzymes that degrades CP via hydrolysis and breakdown into other smaller and intermediatory metabolites such as 3,5,6-trichloro-2-pyridinol (TCP) and diethylthio-phosphoric acid (DETP) etc., (Akbar and Sultan 2016). Bio-bed was formed using peat, andisol, straw and layer of grasses mixed with soil and treated along with the hydrolytic enzymes to mimic the natural environmental degradation of the pesticide (Fernandez

et al. 2012; Tortella et al. 2012). *Flavobacterium* sp. ATCC 27551, *Alcaligen faecalis*, *Arthrobacter* sp., *Klebsilla* sp., *Paracoccus* sp., *Enterobacter* sp., and *Saccharomyces cerevisiae, Aspergillus* sp., *Trichoderma* sp., *Fusarium* sp., *Phanerochaete chrysosporium, Aspergillus terreus*, *Verticillium* sp. are few CP degrading bacterium and fungus strains respectively (Li et al. 2008; John and Shaike 2015; Gilani et al. 2010). *Plesiomonas sp*. M6 was the first bacterial strain from which organophosphate hydrolase (mph) gene was isolated and cloned using *Sphingomonas* sp. strain Dsp-2 and *Stenotrophomonas* sp. strain YC-1 for degradation of CP and its toxic intermediates. The alternate degradation techniques utilizes immobilized enzymes such as lipases, β-glucosidases, lactases combined with nanoparticles to improve the degradation rate of CP. Laccase enzyme immobilized using chitosan as crosslinking agent upon the magnetic iron nanoparticles escalates the degradation of CP (Das et al. 2017).

Photocatalytic degradation process using nanoparticles and nanocomposites are more fascinating as they are rapid and efficient than the existing other degradation routes. The effective photocatalytic degradation of CP was reported by TiO_2 nanoparticles with and without bacterial strains (Budarz et al. 2019). *Carica papaya* mediated co-reduced bimetallic silver/copper nanocatalyst with tentacle like morphology and its application with removal of CP from waste water into lesser toxic product such as diethylthiophosphate (DETP) and 3,5,6-trichloro-2-pyridinol (TCP) (Rosbero and Camacho 2017). Hydrothermal synthesis of hetero junction CuS-$Bi_2O_2CO_3$ system mediated by KCl and urea and the one-pot synthesized novel ternary CuO/TiO2/PANI nanocomposite were recorded with superior photocatalytic degradation of CP under visible light illumination (Majhi et al. 2018). The improved degradation efficiency by photo luminescence process is due to the reduction of narrow band energy gap (2.0 eV) thereby preventing the recombination of the photon generated charges (Nekooie et al. 2021). The mechanism behind photocatalytic degradation of CP with Fe_3O_4 and WS2 nanoparticles immobilized on the mesoporous silica under UV light was low recombination rate of electron-hole pairs (Merci *et al.* 2020). Coated graphene nano-platelets (GNPs) and zirconium vanadate (ZrV_2O_7) system with very least band gap system have higher efficiency of degradation than bare ZrV_2O_7 alone. The hydroxyl radicals and the holes generated were the highly reactive factor for the degradation of the CP in the wastewater (Samy et al. 2020).

Studies on various factors that contributes to the effective degradation of CP were investigated. Moisture, pH, type and load of microbial strain, temperature, concentration of CP, nature of the soil and the type of irradiation source were found to be the most important driving factors for effective degradation activity of the different catalysts (Racke et al. 1996; Singh et al. 2006; Hossain et al. 2013). In this study, novel phyto-source mediated, one-pot co-reduction produced reduced graphene oxide-silver nanoparticles composite was synthesized, characterized for its morphology, functional group and evaluated for its antimicrobial activities. The degradation of the chlorpyrifos was investigated under adsorption and photocatalytic process. The sunlight induces two process with the nanocomposite as excitation of the silver plasmons and the conductive stacked rGO where both enhances the separation of the charged groups in the pesticide and instigates the oxidative degradation of the organophosphate backboned pesticide CP. The various factors that affects the degradation were also studied and optimized.

Materials And Methodology

All the analytical grade chemicals such as graphite powder, silver nitrate, potassium permanganate, acids, organic solvents etc., were purchased from the LOBA chemicals, Mumbai, India. Fresh *Curcubita maxima* leaves and chlorpyrifos were procured from the Chennai local market.

Graphene oxide synthesis using modified hummer's method

Graphene oxide (GO) was synthesized from graphite powder following modified Hummer's method (Yadav et al. 2018). Briefly, 2 g of graphite powder and 2 g of sodium nitrate in 100 ml of concentrated H_2SO_4 was taken in a conical flask and kept in an ice bath and subjected to constant stirring for 2 h. About 14.6 g of $KMnO_4$ was added slowly and periodically to the reaction mixture under continuous stirring at temperatures of 0 – 4 °C. 180 ml of deionized water was slowly added to the stirring setup and stirring was continued until the solution turns into dark brown. 10 ml of 30 % H_2O_2 was added to terminate the reaction confirmed and 110 ml of double distilled water was added for dilution turns the entire suspension into dark yellow color. The stirring setup was switched off and the solution was subjected to centrifugation at 5000 rpm for 5 min. The pellet was taken for continuous 2-3 consecutive wash cycles using dilute HCl, deionized water and ethanol. The produced GO was dried at 40 °C for 4 h (Upadhyay et al. 2015; Esencan and Filiz 2020).

Preparation of *Curcubita maxima* leaf extract

Curcubita maxima leaf extract was used to prepare reduced graphene oxide (rGO) & silver nanoparticles (AgNPs) based on its properties like cheap, easily available, chemical and medicinal property. Fresh leaves were obtained from local farming lands. Leaves surface were thoroughly washed and cleaned thrice with double distilled water and air-dried at room temperature. Leaves weighing 20 g were cut into smaller pieces and boiled for 20 min in a 250 ml flask along with 100 ml of deionized water. The obtained extract was cooled and filtered using Whatman No.1 filter paper and stored at 4 °C and were used for further process (Karthik et al. 2020a; Karthik et al. 2021).

One-pot green synthesis of reduced graphene oxide - silver nanocomposite

100 mg of dried GO synthesized using hummer's method along with 100 mg of $AgNO_3$ was added to 200 ml of distilled water and subjected to magnetic stirring for 2 h at 90 °C. 20 ml of the prepared plant extract was added to the suspension and continued with the stirring for 3 h. The stirring was switched off and the solution was centrifuged at 5000 rpm for 10-15 min. The rGO-AgNP pellet was dried and stored for further studies (Karthik et al. 2020b).

Characterization studies

The synthesized GO and rGO-AgNP composite was characterized initially to confirm the synthesis using systronics 2202 – UV-visible double beam spectrophotometer in the range of 200- 600 nm. The surface morphology of the composite was characterized by scanning electron microscopy (SEM) operated at

voltage of 15 kV using the powdered sample. The functional groups that were present in the GO & rGO-AgNP samples were detected using Perkin Elmer system Fourier transform infrared (FTIR) spectrophotometer in the wave number ranging 4000 - 450 cm^{-1} with a resolution of 1.0 cm^{-1}. The crystal nature of the synthesized GO & rGO-AgNP sample were identified by measuring the diffraction intensity of the nanocomposite at 2 theta angles ranging from 10˚ - 80˚ using Pert MPD X-ray diffractometer with Cu-Kα radiation working at 40 kV and 30 Ma (Karthik et al. 2021; Karthik et al. 2019).

Antimicrobial studies – zone inhibition assay

The antimicrobial activity of the synthesized nanocomposite was studied using inhibition zone assay. Briefly, 100 µl of *E. coli, B. subtilis* and *S. cerevisiae* were inoculated overnight in Luria broth (LB) medium and spread using L-glass rod on nutrient agar plate. The plate was punctured and rGO-AgNP nanocomposite were loaded in the well. It was kept for overnight incubation at 37 °C and the inhibition zone was calculated on the next day after 24 h of incubation comparing with ampicillin as a standard (Karthik and Radha 2016).

Adsorption and photocatalytic degradation studies

The degradation efficiency of synthesized rGO-AgNP composite on chlorpyrifos (CP) was investigated by the adsorption process under room temperature and photocatalytic process under direct sunlight respectively.

Effect of CP concentration and time

The optimal concentration of pesticide at which the maximum percentage of adsorption and photocatalysis takes place were studied (Majhi et al. 2018). Two batches of chlorpyrifos solution were prepared with varying concentration from 200-5000 ppb and adjusted to same pH, added with same catalyst dosage, and after initial absorbance value of the samples, one batch was kept at room temperature and other batch in sunlight (Karthik et al. 2020b). The samples from batches of adsorption and photocatalysis were drawn periodically and checked for its optical density spectrophotometrically with a period of 15 minutes interval and continued until the OD attains a constant value (Khairnar and Shrivastava 2019).

Effect of pH

The optimal pH at which the highest level of photocatalysis takes place was calculated by varying the pH between the range of 3-11. Other parameters such as time, dose of photocatalyst, concentration of the pesticide were kept constant for all the samples of the batch (Singh et al. 2011).

Effect of photocatalyst dosage

The maximum photocatalyst dosage that corresponds to the higher activity was estimated by taking a range of photocatalyst dosage between 2.5 – 25 mg/ml and keeping other parameters such as pH, time

and pesticide concentration constant (Zangiabadi et al. 2019).

The removal of CP was calculated by using the formula

Adsorption efficiency, D (%) = $[(A_0 - A_T) / A_0] \times 100$

A_0 = Initial absorbance value

A_T = Absorbance value at time T

Adsorption isotherm

The widely used adsorption isotherms such as Langmuir and Freundlich isotherm was fitted with the photocatalytic adsorption and the best fit isotherm was investigated using the determination coefficient (R^2) value.

The linear equation of the Freundlich isotherm was given as,

$\log Q_e = \log K_F + (1/n) \log C_e$

Thus the plot between $\log Q_e$ and $\log C_e$ gives a straight line with slope 1/n and y-intercept $\log K_F$ where Q_e – equilibrium concentration of the pesticide adsorbed per unit adsorbent mass (mg/g), C_e – Concentration of the pesticide (mg/L), K_F and 1/n are adsorption constants that corresponds to the capacity and intensity of the system.

The linear equation of the Langmuir II isotherm was given by,

$1/Q_e = 1/ (K_L.Q_m) . 1/C_e + 1/Q_m$

Thus, a plot between $1/Q_e$ versus $1/C_e$ gives a straight line with slope of $(1/K_L.Q_m)$ and y-intercept value $(1/Q_m)$.

Where Q_e – concentration of the pesticide adsorbed at equilibrium condition (mg/g), C_e - concentration of the pesticide adsorbed (mg/L) and K_L, Q_m are the adsorption constants.

Results And Discussion

UV-vis spectroscopy analysis

The GO and rGO-AgNP was confirmed by UV-vis spectroscopy (Fig.1). The UV-vis spectra of GO shows characteristic peak at 230 nm and a small shoulder peak 300 nm correspond to the л-л* transition from aromatic C=C bonds and the n-л* transition of C□O bonds, respectively (Wazir and Kundi 2016). The rGo-Ag spectrum shows characteristics peak of both rGO as well as Ag (Fig.1). The peaks at 270 and 410 nm confirms the co-reduction of GO to rGO and $AgNO_3$ to AgNPs by *Curcubita maxima* leaf extract

simultaneously. The peak at 270 nm is a result of bathochromic shift (red shift) in the peak from 230 nm after reduction of GO to rGO and also restoration of sp^2 carbon network in the structure. The absorption peak at 410 is attributed to the characteristic of the surface plasmon resonance of AgNPs, indicating the presence of AgNPs in the synthesized product (Andrijanto et al. 2016; Zhu et al. 2021). This result clearly indicated that rGO and Ag is synergistically produced by the co-reduction of GO to rGO and $AgNO_3$ to AgNPs by *Curcubita maxima* leaf extract (Zhang et al. 2017; Gurunathan et al. 2015; Chettri et al. 2017).

Fourier transform infrared spectroscopy (FTIR) analysis

Fig. 2 depicts the FTIR spectrum of GO and rGO-Ag nanocomposite respectively. The peaks at 1629 and 3398 cm^{-1} correspond to the stretching vibrations of C=C and hydroxyl groups. The bands at 1714 cm^{-1} and 1050 cm^{-1} region is due to the C=O stretching vibrations of a carbonyl group and C-O stretching vibrations respectively. These peaks indicate the presence of various oxygen functional groups bonded to GO. After the co-reduction of GO and $AgNO_3$, the formation of rGO-AgNp composite leads to changes in the absorption features of the FTIR spectrum. The intensity of the peaks near 1714 and 1050 cm^{-1} in the spectrum got reduced when compared to GO indicates the reduction of GO to RGO by leaf extract. Besides, the peak at 1629 cm^{-1} assigned to the C=C group is retained as such clearly indicates the restoration of graphitic framework of GO. The bands at 2924, 2856, 1629, 1377, 601 cm^{-1} indicates the presence of capping agents present with the nanoparticles. Bands at 2924 and 2856 region arising from C-H stretching of aromatic compound were observed. In addition, the absorption bands at 3421 and 1383 cm^{-1} clearly confirms the presence and coating of silver nanoparticles on the rGO surface (Zhang et al. 2017; Shao et al. 2015; Sun et al. 2015; Kavinkumar et al. 2017).

Scanning electron microscopy (SEM) analysis

The morphological features of the synthesized composite was characterized by scanning electron microscopy analysis. The following figures 3 (a) and 3 (b) of the phyto-synthesized composite are the corresponding images taken at probe distance of 200 µm and 10 µm respectively.

Fig 3 (a) shows the spherical structure of the smaller composite particle with the stacking and also the agglomeration of elongated larger particles at higher concentration and Fig 3 (b) depicts the deposition of the silver nanoparticles over the stacks of rGO, confirms the formation of nanocomposite with successful simultaneous green reduction of Ag^+ and GO by the *Curcubita maxima* leaf extract (Zhang et al. 2017; Kavinkumar et al. 2017; Moghayedi et al. 2020; Zhou et al. 2019).

Energy dispersive x-ray spectroscopy analysis

The characteristic diffraction peak of dried and powdered GO upon XRD analysis at 11.4° with an interlayer spacing of 7.93 Å (Moosa et al. 2021). Peak at 28.64° corresponds to the residual graphite traces present in the sample and peak at 63.48° represents the traces of Cl, from the subsequent wash cycle carried out to the GO using HCl. The successful reduction of GO to rGO was confirmed by the

characteristic peak at 28.90° indicating the effective reduction potential by the leaf extract of *Curcubia maxima*. The peaks at the 38.52°, 46.5°, 54.9°, 64.48° and 77.80° designated to the (111), (200), (220), (311) planes confirms the face centered cubic crystallinity of the silver nanoparticles (Karthik et al. 2020b; Ansari et al. 2018). The peaks at 32.64° and 57.92° are reflected due to the organic molecules present in the reductant source (Al Aboody 2019; Vijayan et al. 2019).

Antimicrobial studies

Antimicrobial activity of the synthesized composite was tested against standard antibiotic through zone inhibition assay and the zone of inhibition was calculated. *Escherichia coli* (gram- negative), *Bacillus subtilis* (gram-positive) and *Saccharomyces cerevisiae* (yeast) are tested against the composite and found to possess antimicrobial activity.

Table 1: Antimicrobial activity of the synthesized nanocomposite

19. No	Microbial strain	Zone of Inhibition (diameter in mm)	
		Ampicillin	Nanocomposite
1.	*Escherichia coli*	16 ± 0.6	22 ± 0.5
2.	*Bacillus subtilis*	15.5 ± 0.5	21 ± 0.4
3.	*Saccharomyces cereviseae*	16.5 ± 0.5	23 ± 0.5

rGO-AgNP possess stronger inhibition with fungal cell wall as the reactive oxygen species synthesized by the rGO sheets have capability to interact with the several organic functional groups present in chitin and other cellular polysaccharides (Sawangphruk et al. 2012). Treatment with Ag+ ions impacts with the replicative property of the DNA and inactivate the expression of various cellular, ribosomal proteins, membrane-bound and different other enzymes involved in the ATP production cycles (Kim et al. 2012). As reported by Paredes et al. 2014, gram-positive *E. coli* strains have higher affinity towards silver nanoparticles due to the layer of lipopolysaccharide with negatively charged teichoic acid and peptidoglycan layers which attracts more positively charged silver ions and thus with higher diameter of zone of inhibition (ZOI) than the gram negative *B. subtilis* strain with comparatively lesser ZOI diameter (Paredes et al. 2014). The silver ion interaction with phosphor and sulfur containing groups of the plasma membrane increases its susceptibility and thereby the leakage of the cellular contents (Patil and Kim 2017). rGO-AgNP composite gets conjugated with the cellular membrane, interfere with the signaling pathways for cellular growth and also reduced cell viability, division and increased DNA leakage and consequent death (Bai et al. 2016).

Adsorption and photocatalysis studies:

Effect of time

The degradation efficiency of synthesized rGO-AgNP composite was investigated by varying the chlorpyrifos (CP) concentration under adsorption (dark reaction) and photocatalytic (sunlight) environment. The results indicates the maximum degradation rate of 51 % and 76 % is observed at 105 min in both adsorption and photocatalytic condition respectively. The trend of the graphs are represented in fig 5. The CP did not undergo efficient degradation under normal adsorption process when compared to photocatalytic irradiation. At initial stage the comparative analysis between adsorption and photocatalysis, shows that the degradation efficiency differs almost by 50 % in case of photocatalysis than adsorption. This may be because of the fact that in the presence of visible light, CP degradation was observed to take place with both the influence of catalyst and irradiation energy source. Photocatalysis activates the metal-based photocatalyst by using the energy source from the visible light and promotes advanced oxidation-reduction reactions and charge separation efficiency on the catalyst surface considerably (Bhunia and Jana 2014, da Silva et al. 2021).

A two-step mechanism of removal is proposed with the rGO-AgNP composite for the degradation of halogenated pesticides. The reactive silver present in the rGO-AgNP composite interface reacts with the halogen group of the CP and initiates the degradative pathway followed by the next step of adsorption of the degraded aromatic fragments to the rGO in the composite through stronger π –π electron interaction and weaker hydrogen and van der Waals bonds (Koushik et al. 2016).

Increase in the irradiation time upto 105 min lead to the increase in the degradation efficiency and after which unaltered values of degradation efficiency was observed due to no further degrading radical production. This could also be due to the agglomeration and adsorption of the degraded products to the surface of the photocatalyst and hence 105 min is the optimized time for chlorpyrifos degradation through rGO-AgNP composite synthesized using *Cucurbita maxima* (Nekooie ey al. 2021; Khairnar and Shrivastava 2019).

Effect of initial pesticide concentration

The effect of initial concentration of the pesticide with the adsorption and photocatalytic degradation was studied by varying concentration in the range of 200-5000 ppb. It is evident that the percentage of the degradation is higher with photocatalysis than with adsorption (Fig. 5). The concentration of 1 ppm has higher percentage of comparative degradation, 75.5 % degradation in photocatalysis and 49.48 % degradation in adsorption was observed. Initially the increase in the percentage of degradation was found until optimal level as the active electron-hole pair species produced by the sunlight illumination was sufficient for degradation. As the pesticide concentration increases to higher than optimal level, the illuminated photocatalyst does not able to produce sufficient OH^- radical and positive hole active species that accounts for the degradation and hence the reduced level of degradation was reported (Zangiabadi et al. 2019; Soltani et al. 2020; Khan et al. 2018; Kgoetlana et al. 2020).

Effect of pH

The CP solution with pH range of 3-11 with optimized time and pesticide concentration was observed with the following results in Fig 6.

The observed results showed that at pH 7 highest percentage of the degradation of the pesticide takes place, followed by pH 5 and 3 as observed with pH 9 and 11 comparatively (Soltani-nehad *et al.* 2019). At acidic pH, the photocatalyst tends to disassemble as Ag^+ ions dissolutes to move from the rGO interface hence with reduced activity whereas at alkaline pH the degradation of pesticide reduction shall be due to the reduced activity of the $OH^{\bullet}$ radical due to its interaction with OH^- and forms water and O^- ion (Nekooie et al. 2021; Zangiabadi et al. 2019; Majhi et al. 2018).

Effect of photocatalyst dosage

For investigating of the effect of the photocatalyst loading, at fixed pH and CP concentration of different load of photocatalyst from 0.25 to 2.5 mg/ml were tested and the following result was obtained.

10 mg /10 ml i.e. 1 mg/ml of the photocatalyst dosage has been found to be optimal level of the adsorbent concentration and beyond which the degradation percentage has tend to decrease gradually. Initially the increase in photocatalyst dose increases the active catalytic centres and activity until optimal level after which photocatalyst aggregation and increased interference with light scattering and improved opacity as well (Nekooie et al. 2021; Soltani et al. 2020).

Adsorption isotherm

The Chlorpyrifos adsorption by the rGO-AgNP composite was checked for fitting into the Langmuir and Freundlich isotherms (Karthik et al. 2020b; Khairnar and Shrivastava 2019; Soltani et al. 2020; Kgoetlana et al. 2020).

Langmuir isotherm

The adsorption isotherms were studied by calculating the amount of the pesticide adsorbed per unit mass of nanocomposite adsorbent (q_e) and the equilibrium concentration of the pesticide present in the solution (C_e). From the results calculated from C_e Vs q_e derivatives, it is found that the Langmuir II isotherm fits best to the experimental data. The characteristic linear equation of the Langmuir isotherm is as follows:

$$1/q_e = 1/(K_L q_m)\ \ 1/C_e + 1/q_m$$

Where K_L is the Langmuir constant (g/L) and q_m is the maximum adsorption capacity of pesticide by the nanocomposite (mg/g). From the plot between $1/C_e$ vs $1/q_e$, (Fig 1) the Langmuir constants of the experiment are reported as follows.

The Langmuir adsorption characteristic linear equation is y = 321.8x + 0.2554 and regression coefficient R^2 is 0.994, which is approximately more closer to linear form and the Langmuir adsorption parameters

are found as the monolayer composite's maximal adsorption q_m is 3.92 mg/g and the Langmuir equilibrium constant K_L as 7 X 10^{-4} (g/L) .

Seperation factor (R_L):

R_L is a dimensionless constant that has significant role in understanding the Langmuir isotherm. The Langmuir separation factor characteristic equation is

$R_L = 1/ (1+K_L C_O)$

Where R_L is the separation constant (no unit), K_L is the Langmuir constant (g/L) and Co is the initial pesticide concentration (mg/L). The separation factor calculation for the experiment with optimized nanocomposite amount and pH at varying concentration of pesticides follows the trend in Fig 9. The range of R_L values lies between 0.22 - 0.88 which indicates the favorable adsorption of pesticide upon the rGO-AgNP.

Freundlich Isotherm

Freundlich isotherm is another linear isotherm which considers the logarithmic values of the concentration of the pesticide in the solution at equilibrium (Ce) and the amount of pesticide adsorbed to the surface of the adsorbent (Qe). From Freundlich characteristic equation, $q_e = K_F C_e^{1/n}$ and its linear logarithmic value equation, $\log q_e = 1/n \log C_e + \log K_F$, the Freundlich isotherm parameters can be calculated. Where C_e = equilibrium concentration of the pesticide (mg / L), q_e = pesticide amount adsorbed per unit mass of the nanocomposite adsorbent (mg / g), K_F and 1/n are the adsorption isotherm related constants that corresponds to the capacity and intensity of adsorption. log Ce vs. Log Qe plot gives Freundlich isotherm equation and the regression coefficient R^2 is found to be 0.959. The Freundlich isotherm constants K_F is 2.88 mg/g of pesticide adsorbed per unit of nanocomposite and n is 1.42, greater than 1, that confirms the stronger interaction between adsorbent and adsorbate (Karthik et al. 2020b).

Table: Adsorption kinetics parameters

Isotherm	Parameter	Value
Langmuir Isotherm	Q_m (mg/g)	3.92
	K_L (g/L)	$7X10^{-4}$
	R^2	0.994
Freundlich Isotherm	K_F (mg/g)	2.88
	n (L/mg)	1.42
	R^2	0.959

Conclusion

The rGO-AgNP was synthesized in one-pot through phytosynthesis from leaf extract of *curcubita maxima* was confirmed primarily by UV-vis spectroscopy and the arrangement of the composite was found to be stacked rGO within which spherical silver was incorporated as confirmed by SEM analysis. FTIR shows the interactive bonds between phytoreductant and composite. XRD data gives information on the planar lattice information. The composite is found to possess anti-microbial activity against gram-positive strain *B. subtilis*, gram-negative bacterial strain *E. coli* and fungal strain *S. cerevisiae.* The rGO-AgNC activity of photocatalysis was optimized with the adsorbent dosage, pH, time and pesticide concentration separately. The photocatalysis was found to be with nearly ideal fit to Langmuir isotherm than freundlich isotherm. This needs to be investigated further for other different improvisations to completely degrade the harmful organophosphate pesticide from the biological ecosystem and its food chain accumulation.

Declarations

Ethical Approval

This article does not contain any studies involving animals performed by any of the authors.

Consent to Participate

This article does not contain any patient/study participant/parent/guardian/next of kin.

Consent to Publish

The authors give their consent for the publication of identifiable details, which can include images and other details within the text to be published in the journal.

Authors Contributions

All authors contributed to the study conception and design. All authors read and approved the final manuscript.

Dr. Karthik Chinnappa: Conceptualization, Methodology, Supervision, Resources

Mr. Punnaivalavan Karuna Ananthai: Investigation, Formal analysis, Writing - Original Draft

Dr. Pandi Prabha Srinivasan: Writing - Review & Editing, Visualization

Ms. Caroline Dharmaraj Glory Bai: Writing - Review & Editing, Visualization

Funding

The authors declare that no funds, grants, or other support were received during the preparation of this manuscript.

Competing Interests

The authors have no relevant financial or non-financial interests to disclose.

Availability of data and materials

All data generated or analysed during this study are included in this manuscript.

References

1. Akbar S, Sultan S (2016) Soil bacteria showing a potential of chlorpyrifos degradation and plant growth enhancement. Braz J Microbiol 47:563-570. https://doi: 10.1016/j.bjm.2016.04.009
2. Al Aboody MS (2019) Silver/silver chloride (Ag/AgCl) nanoparticles synthesized from Azadirachta indica lalex and its antibiofilm activity against fluconazole resistant *Candida tropicalis*. Artif Cells Nanomed Biotechnol 47(1):2107-13. https://doi.org/10.1080/21691401.2019.1620257
3. Andrijanto E, Shoelarta S, Subiyanto G, Rifki S (2016, April) Facile synthesis of graphene from graphite using ascorbic acid as reducing agent. In *AIP* Conference Proceedings (Vol. 1725, No. 1, p. 020003). AIP Publishing LLC.
4. Ansari Z, Saha A, Singha SS, Sen K (2018) Phytomediated generation of Ag, CuO and Ag-Cu nanoparticles for dimethoate sensing. J Photochem Photobiol A 367:200-211.https:// DOI: 10.1016/j.jphotochem.2018.08.026
5. Bai RG, Muthoosamy K, Shipton FN, Pandikumar A, Rameshkumar P, Huang NM, Manickam S (2016) The biogenic synthesis of a reduced graphene oxide–silver (RGO–Ag) nanocomposite and its dual applications as an antibacterial agent and cancer biomarker sensor. RSC Adv 6(43):36576-87. https://doi.org/10.1039/C6RA02928K
6. Bhunia SK, Jana NR (2014) Reduced graphene oxide-silver nanoparticle composite as visible light photocatalyst for degradation of colorless endocrine disruptors. ACS Appl Mater Interfaces

6(22):20085-20092. https://doi.org/10.1021/am505677x

7. Bootharaju MS, Pradeep T (2012) Understanding the degradation pathway of the pesticide, chlorpyrifos by noble metal nanoparticles. Langmuir 28(5):2671-2679. https:// doi: 10.1021/la2050515.
8. Budarz JF, Cooper EM, Gardner C, Hodzic E, Ferguson PL, Gunsch CK, Wiesner MR (2019) Chlorpyrifos degradation via photoreactive TiO_2 nanoparticles: assessing the impact of a multi-component degradation scenario. J Hazard Mater 372:61-68. https:// doi: 10.1016/j.jhazmat.2017.12.028
9. Chettri P, Vendamani VS, Tripathi A, Singh MK, Pathak AP, Tiwari A (2017) Green synthesis of silver nanoparticle-reduced graphene oxide using Psidium guajava and its application in SERS for the detection of methylene blue. Appl Surf Sci 406:312-318. https://doi.org/10.1016/j.apsusc.2017.02.073
10. da Silva W L, Druzian D M, Oviedo L R, Muraro P C L and Oviedo V R (2021) Silver Nanoparticles for Photocatalysis and Biomedical Applications. In Silver Micro-Nanoparticles-Properties, Synthesis, Characterization, and Applications. IntechOpen. DOI: 10.5772/intechopen.95922
11. Das A, Singh J, Yogalakshmi KN (2017) Laccase immobilized magnetic iron nanoparticles: fabrication and its performance evaluation in chlorpyrifos degradation. Int Biodeterior Biodegradation 117:183-189. https:// doi:10.1016/j.ibiod.2017.01.007
12. Deb N, Das S (2013) Chlorpyrifos toxicity in fish: a review. Curr World Environ 8(1):77-84. http://dx.doi.org/10.12944/CWE.8.1.17
13. Esencan Turkaslan B, Filiz Aydin M (2020) Optimizing parameters of graphene derivatives synthesis by modified improved Hummers. Mathematical Methods in the Appl Sci https://doi.org/10.1002/mma.6704
14. Fernández-Alberti S, Rubilar O, Tortella GR, Diez MC (2012) Chlorpyrifos degradation in a Biomix: Effect of pre-incubation and water holding capacity. J Soil Sci Plant Nutr 12(4):785-799.http://dx.doi.org/10.4067/S0718-95162012005000032
15. Gilani ST, Ageen M, Shah H, Raza S (2010) Chlorpyrifos degradation in soil and its effect on soil microorganisms. J Anim Plant Sci 20(2):99-102.
16. Gurunathan S, Han JW, Park JH, Kim E, Choi YJ, Kwon DN, Kim JH (2015) Reduced graphene oxide–silver nanoparticle nanocomposite: a potential anticancer nanotherapy. Int J Nanomedicine 10:6257.https:// doi: 10.2147/IJN.S92449
17. Hossain MS, Fakhruddin AN, Chowdhury MA, Alam MK (2013) Degradation of chlorpyrifos, an organophosphorus insecticide in aqueous solution with gamma irradiation and natural sunlight. J Environ Chem Eng 1(3):270-274. https://doi.org/10.1016/j.jece.2013.05.006 https://doi.org/10.1016/j.apsusc.2018.06.051
18. John EM, Shaike JM (2015) Chlorpyrifos: pollution and remediation. Environ Chem Lett 13(3):269-291. https://doi.org/10.1007/s10311-015-0513-7

19. Karthik C, Anand K, Leecanro M, Preethy KR (2019) Phytosynthesis of silver nanoparticles using *Calotropis gigantea* flower extract and its antibacterial activity. JoNSNEA.;9:53-60.
20. Karthik C, Caroline DG, Priya MD, Prabha SP (2021) Synthesis, Characterization of Ag-SiO_2 Nanocomposite and Its Application in Food Packaging. J Inorg Organomet Polym Mater 31(6):2532-2541. https://doi.org/10.1007/s10904-020-01853-7
21. Karthik C, Radha KV (2016) Silver nanoparticle loaded activated carbon: An escalated nanocomposite with antimicrobial property. Orient J Chem 2016 Mar 1;32:735-741. http://dx.doi.org/10.13005/ojc/320182
22. Karthik C, Suresh S, Mirulalini S, Kavitha S (2020) A FTIR approach of green synthesized silver nanoparticles by *Ocimum sanctum* and *Ocimum gratissimum* on mung bean seeds. Inorg Nano-Met Chem 50(8):606-612. https://doi.org/10.1080/24701556.2020.1723025
23. Karthik C, Swathi N, Caroline DG (2020) Green synthesized rGO-AgNP hybrid nanocomposite–an effective antibacterial adsorbent for photocatalytic removal of DB-14 dye from aqueous solution. J Environ Chem Eng 8(1):103577. https:// DOI:10.1016/j.jece.2019.103577
24. Kavinkumar T, Varunkumar K, Ravikumar V, Manivannan S (2017) Anticancer activity of graphene oxide-reduced graphene oxide-silver nanoparticle composites. J Colloid Interface Sci 505:1125-1133. https://doi.org/10.1016/j.jcis.2017.07.002
25. Kgoetlana CM, Malinga SP, Dlamini LN (2020) Photocatalytic Degradation of Chlorpyrifos with Mn-WO_3/SnS_2 Heterostructure. Catalysts. 10(6):699. https://doi.org/10.3390/catal10060699
26. Khairnar SD, Shrivastava VS (2019) Photocatalytic degradation of chlorpyrifos and methylene blue using α-Bi_2O_3 nanoparticles fabricated by sol–gel method. SN Appl Sci 1(7):1-0. https://doi.org/10.1007/s42452-019-0761-4
27. Khan SH, Pathak B, Fulekar MH (2018) Synthesis, characterization and photocatalytic degradation of chlorpyrifos by novel Fe: ZnO nanocomposite material. Nanotechnol Environ Eng 3(1):1-4. https://doi.org/10.1007/s41204-018-0041-3
28. Kim SW, Jung JH, Lamsal K, Kim YS, Min JS, Lee YS (2012) Antifungal effects of silver nanoparticles (AgNPs) against various plant pathogenic fungi. Mycobiology 40(1):53-8. https://doi.org/10.5941/MYCO.2012.40.1.053
29. Koushik D, Gupta SS, Maliyekkal SM, Pradeep T (2016) Rapid dehalogenation of pesticides and organics at the interface of reduced graphene oxide–silver nanocomposite. J Hazard Mater 308:192-8. https://doi.org/10.1016/j.jhazmat.2016.01.004
30. Li X, Jiang J, Gu L, Ali SW, He J, Li S (2008) Diversity of chlorpyrifos-degrading bacteria isolated from chlorpyrifos-contaminated samples. Int Biodeterior Biodegradation 62(4):331-335.https:// DOI:10.1016/j.ibiod.2008.03.001
31. Majhi D, Bhoi YP, Samal PK, Mishra BG (2018) Morphology controlled synthesis and photocatalytic study of novel CuS-$Bi_2O_2CO_3$ heterojunction system for chlorpyrifos degradation under visible light illumination. Appl Surf Sci 455:891-902.

32. Merci, S., Saljooqi, A., Shamspur, T. and Mostafavi, A (2020) Investigation of photocatalytic chlorpyrifos degradation by a new silica mesoporous material immobilized by WS_2 and Fe_3O_4 nanoparticles: Application of response surface methodology. Appl Organomet Chem *34*(3), p.e5343. https://doi.org/10.1002/aoc.5343
33. Moghayedi M, Goharshadi EK, Ghazvini K, Ahmadzadeh H, Jorabchi MN (2020) Antibacterial activity of Ag nanoparticles/phosphomolybdate/reduced graphene oxide nanocomposite: Kinetics and mechanism insights. Mater Sci Eng B: Solid-State Mater Adv Technol 262:114709. https://doi.org/10.1016/j.mseb.2020.114709
34. Moosa AA, Mahdi ZH, Mutar MA (2021) Preparation of graphene oxide from expanded graphite at different microwave heating times. J Eng Technol Sci 53(3):210305. https:// DOI: 10.5614/j.eng.technol.sci.2021.53.3.5
35. Nekooie R, Shamspur T, Mostafavi A (2021) Novel CuO/TiO2/PANI nanocomposite: Preparation and photocatalytic investigation for chlorpyrifos degradation in water under visible light irradiation. J Photochem Photobiol A 407:113038. https://doi.org/10.1016/j.jphotochem.2020.113038
36. Paredes D, Ortiz C, Torres R (2014) Synthesis, characterization, and evaluation of antibacterial effect of Ag nanoparticles against *Escherichia coli* O157: H7 and methicillin-resistant *Staphylococcus aureus* (MRSA). Int J Nanomedicine 9:1717. https://doi.org/10.1016/j.carbon.2012.06.056
37. Patil MP, Kim GD (2017) Eco-friendly approach for nanoparticles synthesis and mechanism behind antibacterial activity of silver and anticancer activity of gold nanoparticles. Appl Microbiol Biotechnol 101(1):79-92. https://doi.org/10.1007/s00253-016-8012-8
38. Racke KD, Steele KP, Yoder RN, Dick WA, Avidov E (1996) Factors affecting the hydrolytic degradation of chlorpyrifos in soil. J Agric Food Chem 44(6):1582-1592. https://doi.org/10.1021/jf9506141
39. Rosbero TM, Camacho DH (2017) Green preparation and characterization of tentacle-like silver/copper nanoparticles for catalytic degradation of toxic chlorpyrifos in water. J Environ Chem Eng 5(3):2524-2532. https:// DOI : 10.1016/j.jece.2017.05.009
40. Samy M, Ibrahim MG, Alalm MG, Fujii M, Diab KE, ElKady M (2020) Innovative photocatalytic reactor for the degradation of chlorpyrifos using a coated composite of ZrV_2O_7 and graphene nano-platelets. Chem Eng J 395:124974. https://doi.org/10.1016/j.cej.2020.124974
41. Sawangphruk M, Srimuk P, Chiochan P, Sangsri T, Siwayaprahm P (2012) Synthesis and antifungal activity of reduced graphene oxide nanosheets. Carbon 50(14):5156-61. https://doi.org/10.1016/j.carbon.2012.06.056
42. Shao W, Liu X, Min H, Dong G, Feng Q, Zuo S (2015) Preparation, characterization, and antibacterial activity of silver nanoparticle-decorated graphene oxide nanocomposite. ACS Appl Mater Interfaces 7(12):6966-6673. https://doi.org/10.1021/acsami.5b00937
43. Singh BK, Walker A, Wright DJ (2006) Bioremedial potential of fenamiphos and chlorpyrifos degrading isolates: influence of different environmental conditions. Soil Biol Biochem 38(9):2682-2693.https://doi.org/10.1016/j.soilbio.2006.04.019

44. Singh DP, Khattar JI, Nadda J, Singh Y, Garg A, Kaur N, Gulati A (2011) Chlorpyrifos degradation by the cyanobacterium *Synechocystis sp*. strain PUPCCC 64. Environ Sci Pollut Res 18(8):1351-1359.https:// DOI:10.1007/s11356-011-0472-x
45. Soltani-Nezhad F, Saljooqi A, Mostafavi A, Shamspur T (2020) Synthesis of Fe_3O_4/CdS–ZnS nanostructure and its application for photocatalytic degradation of chlorpyrifos pesticide and brilliant green dye from aqueous solutions. Ecotoxicol Environ Saf 189:109886. https://doi.org/10.1016/j.ecoenv.2019.109886
46. Sun XF, Qin J, Xia PF, Guo BB, Yang CM, Song C, Wang SG (2015) Graphene oxide–silver nanoparticle membrane for biofouling control and water purification. Chem Eng Sci 281:53-59. https://doi.org/10.1016/j.cej.2015.06.059
47. Tortella GR, Rubilar O, Castillo M, Cea M, Mella-Herrera R, Diez MC (2012) Chlorpyrifos degradation in a biomixture of biobed at different maturity stages. Chemosphere 88(2):224-228.https:// https://doi.org/10.1016/j.chemosphere.2012.02.072
48. Upadhyay RK, Soin N, Bhattacharya G, Saha S, Barman A, Roy SS (2015) Grape extract assisted green synthesis of reduced graphene oxide for water treatment application. Mater Lett 160:355-358. https://doi.org/10.1016/j.matlet.2015.07.144
49. Vijayan R, Joseph S, Mathew B (2018) Green synthesis of silver nanoparticles using Nervalia zeylanica leaf extract and evaluation of their antioxidant, catalytic, and antimicrobial potentials. Part Sci Technol 37:7, 809-819, DOI: 10.1080/02726351.2018.1450312
50. Wazir AH, Kundi IW (2016) Synthesis of Graphene Nano Sheets by the Rapid Reduction of Electrochemically Exfoliated Graphene Oxide Induced by Microwaves. J Chem Soc Pak 38(1):11-16.
51. Yadav S, Goel N, Kumar V, Tikoo K and Singhal S (2018) Removal of fluoroquinolone from aqueous solution using graphene oxide: experimental and computational elucidation. Environ Sci Pollut Res *25*(3):2942-2957.
52. Yang D, Howard A, Bruun D, Ajua-Alemanj M, Pickart C, Lein PJ (2008) Chlorpyrifos and chlorpyrifos-oxon inhibit axonal growth by interfering with the morphogenic activity of acetylcholinesterase. Toxicol Appl Pharmacol 228(1):32-41. https:// doi: 10.1016/j.taap.2007.11.005.
53. Zangiabadi M, Shamspur T, Saljooqi A, Mostafavi A (2019) Evaluating the efficiency of the GO-Fe_3O_4/TiO_2 mesoporous photocatalyst for degradation of chlorpyrifos pesticide under visible light irradiation. Appl Organomet Chem May;33(5):e4813. https://doi.org/10.1002/aoc.4813
54. Zhang XF, Huang FH, Zhang GL, Bai DP, Massimo DF, Huang YF, Gurunathan S (2017) Novel biomolecule lycopene-reduced graphene oxide-silver nanoparticle enhances apoptotic potential of trichostatin A in human ovarian cancer cells (SKOV3). Int J Nanomedicine 12:7551–7575. https:// doi: 10.2147/IJN.S144161
55. Zhou R, Yin Y, Long D, Cui J, Yan H, Liu W, Pan JH (2019) PVP-assisted laser ablation growth of Ag nanocubes anchored on reduced graphene oxide (rGO) for efficient photocatalytic CO_2 reduction. Prog Nat Sci Mater Int 29(6):660-6. https://doi.org/10.1016/j.pnsc.2019.11.001

56. Zhu J, Ni H, Hu C, Zhu Y, Cai J, Liu S, Gao J, Yang H, Liu H (2021) Rapid synthesis and characterization of silver-loaded graphene oxide nanomaterials and their antibacterial applications. R Soc Open Sci 8(2):201744. https:// doi: 10.1098/rsos.201744

Figures

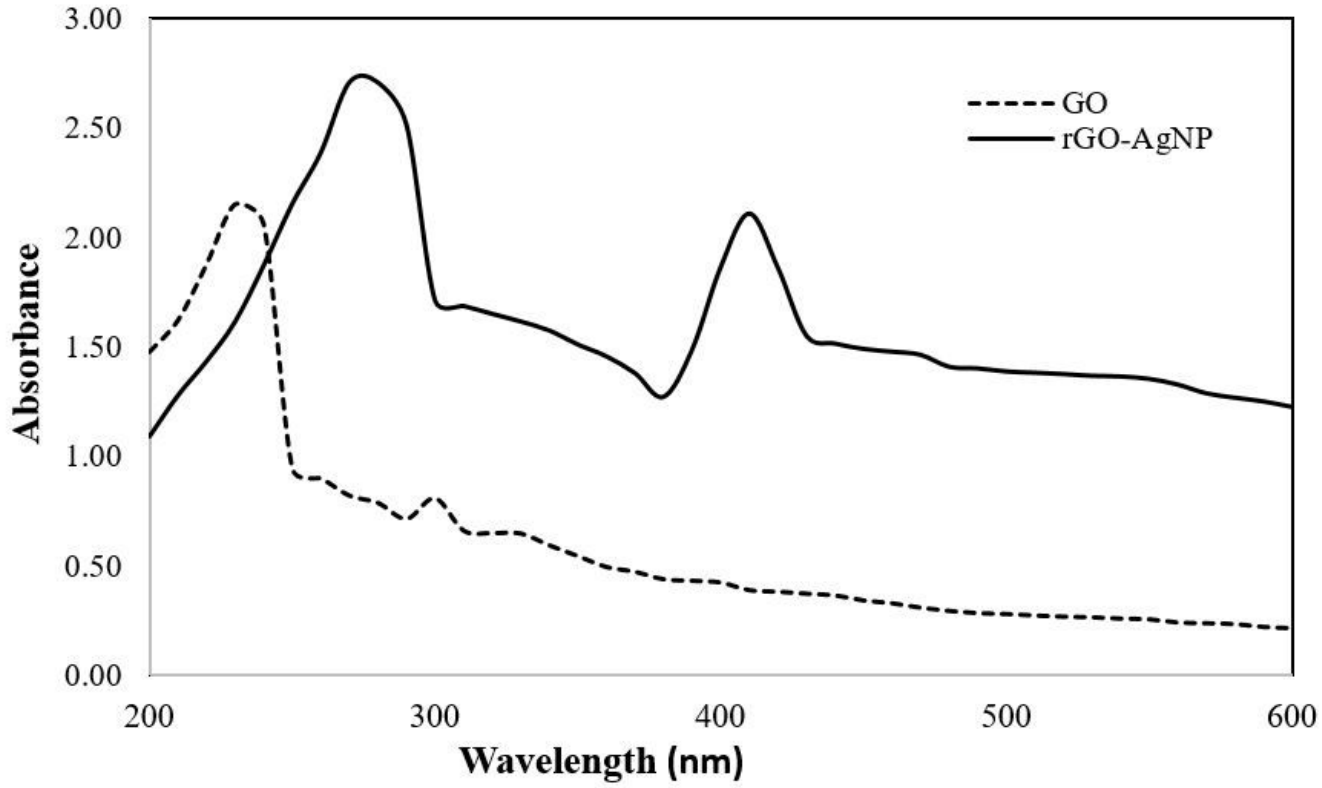

Figure 1

UV-vis spectra of GO and rGo-AgNP

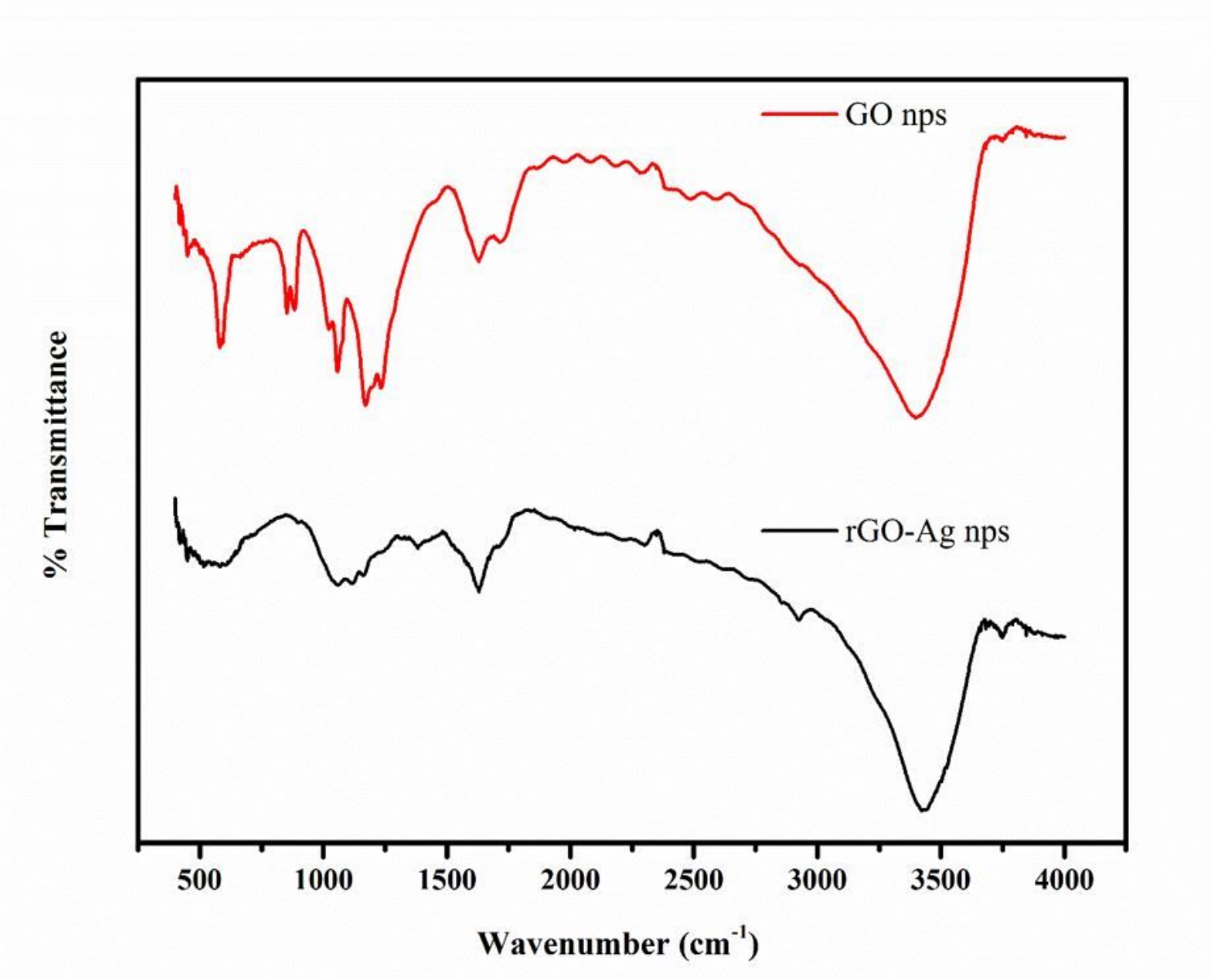

Figure 2

FTIR spectra of GO and rGo-AgNP

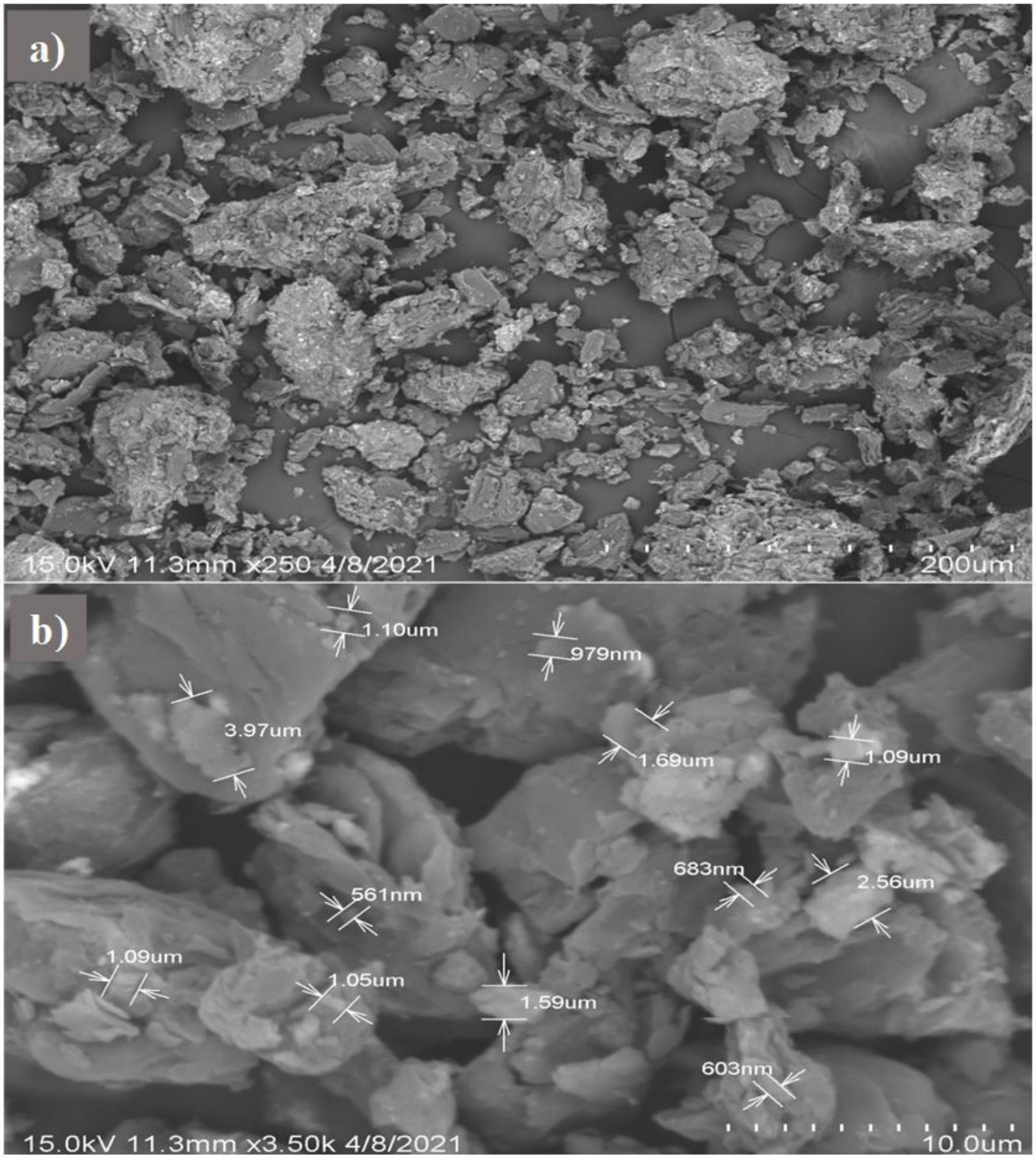

Figure 3

Morphology of rGo-AgNP by SEM analysis

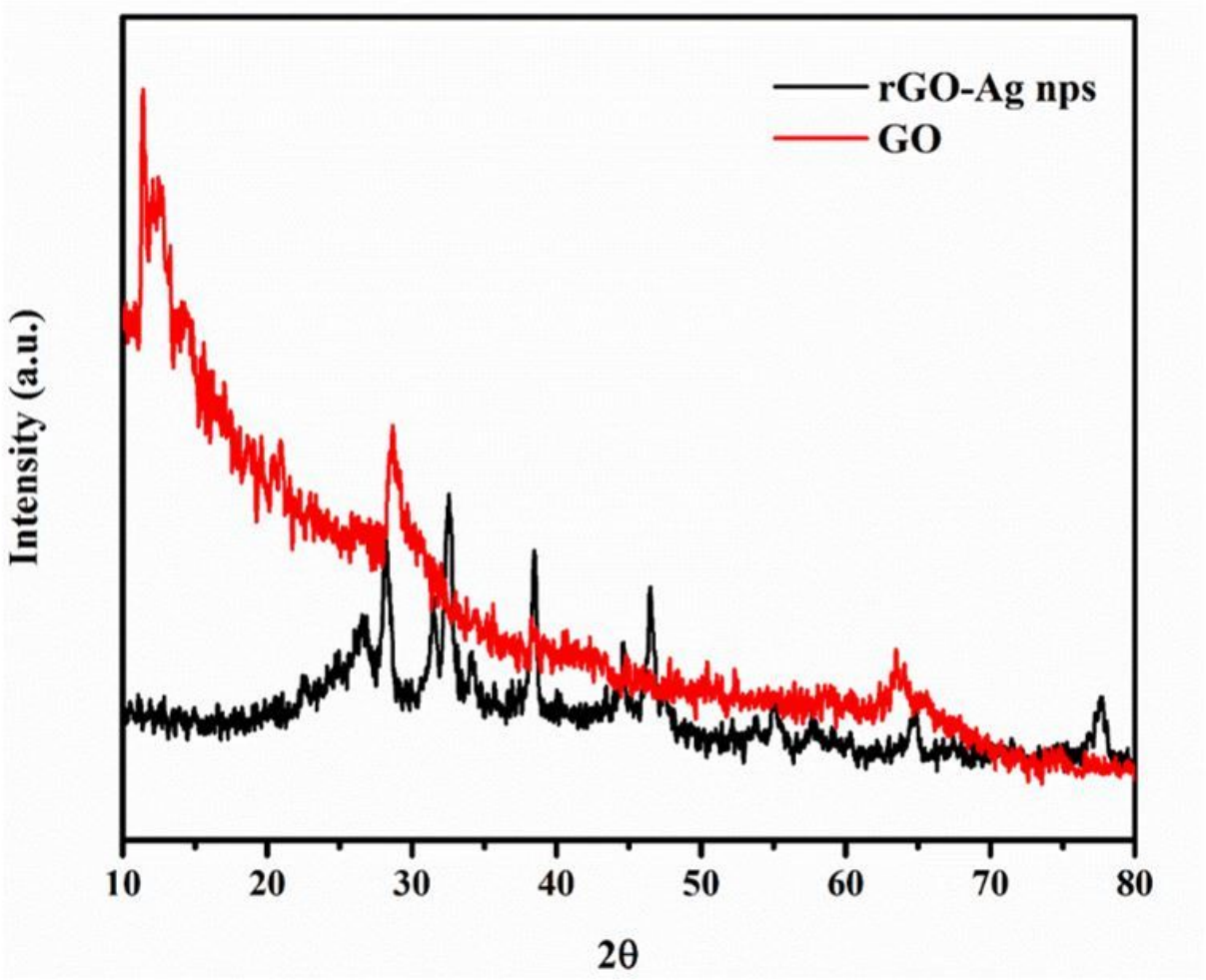

Figure 4

XRD of GO and rGo-AgNP

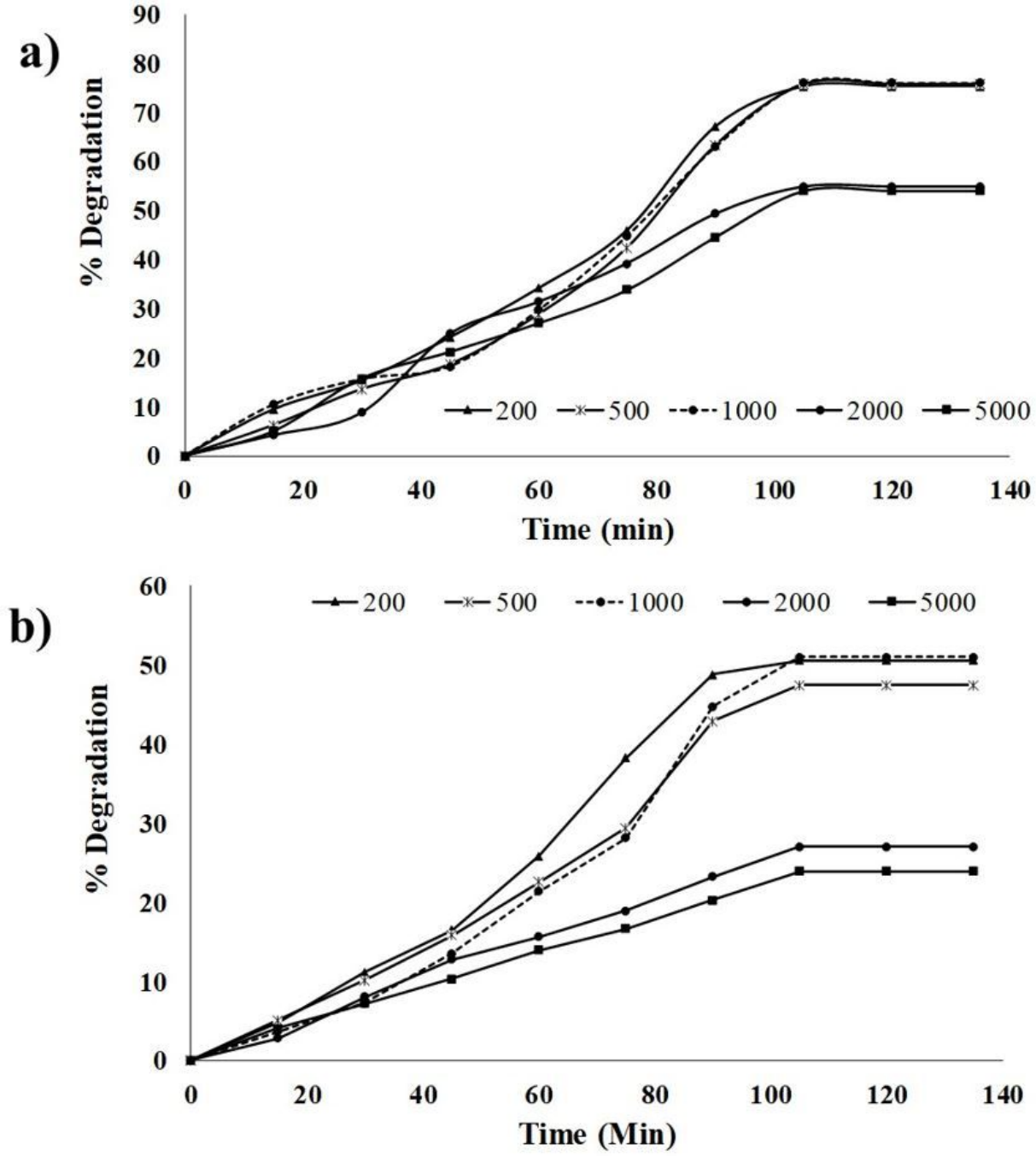

Figure 5

(a) Adsorption and (b) Photocatalytic degradation of chlorpyrifos by rGO-AgNP nanocomposite

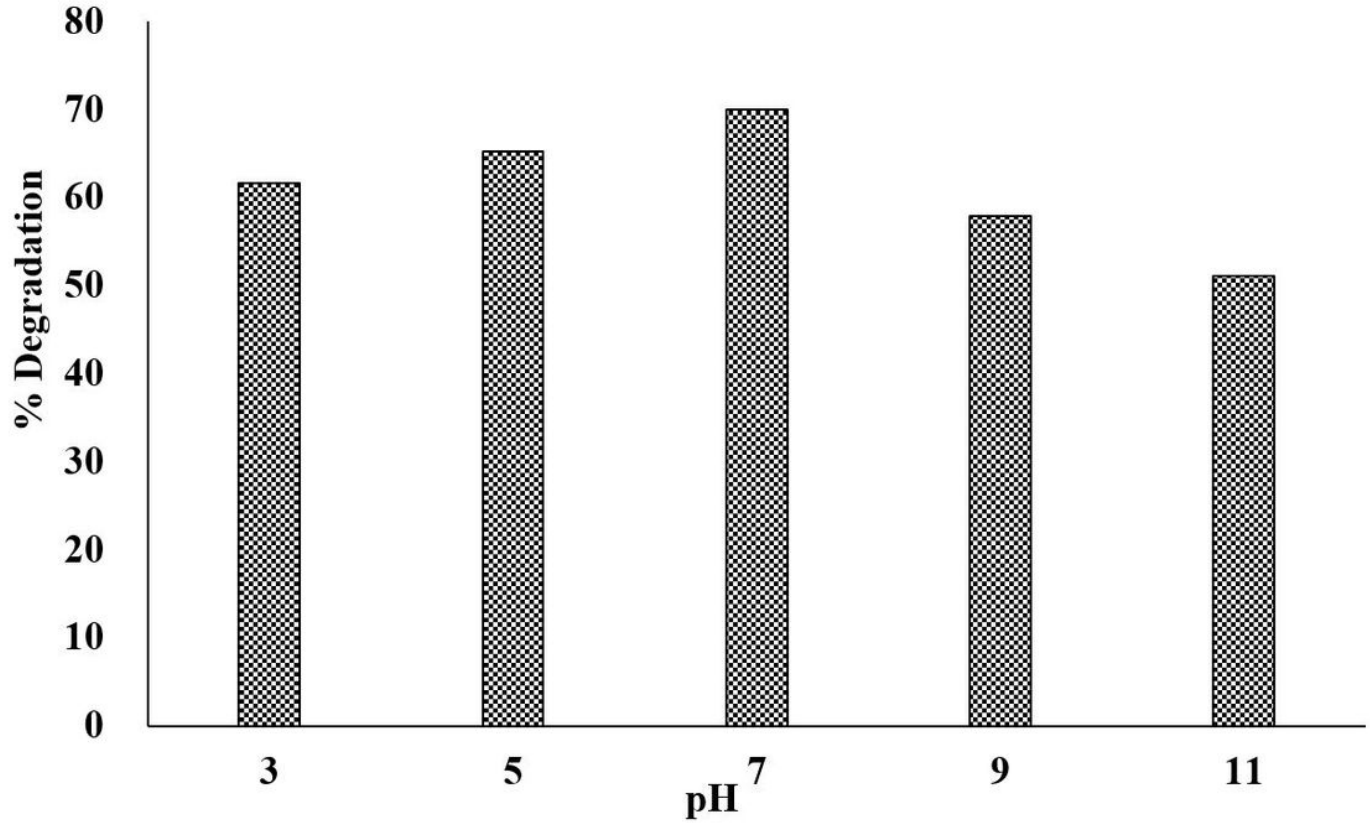

Figure 6

Effect of pH photocatalytic degradation of chlorpyrifos by rGO-AgNP nanocomposite

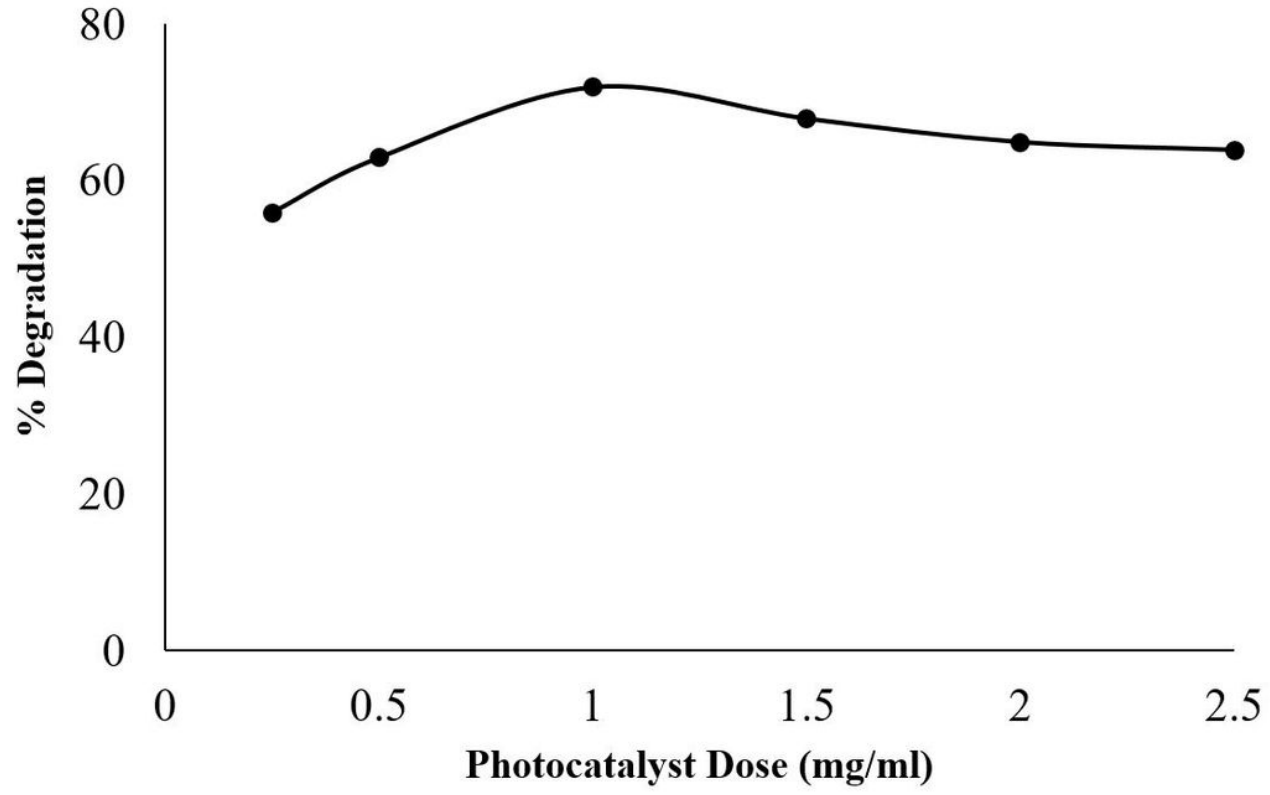

Figure 7

Effect of photocatalyst dosage on photocatalytic degradation of chlorpyrifos by rGO-AgNP nanocomposite

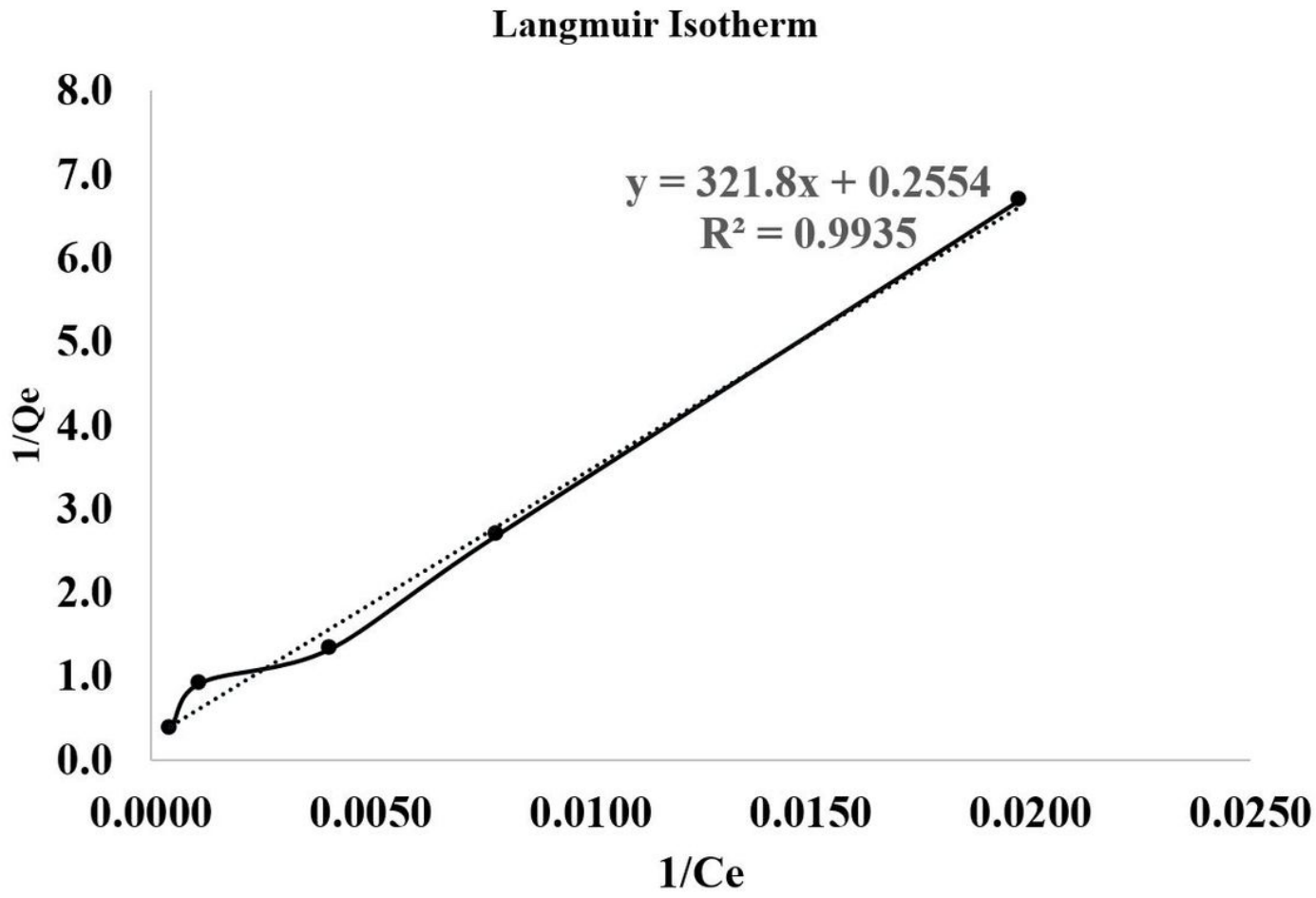

Figure 8

Langmuir Isotherm

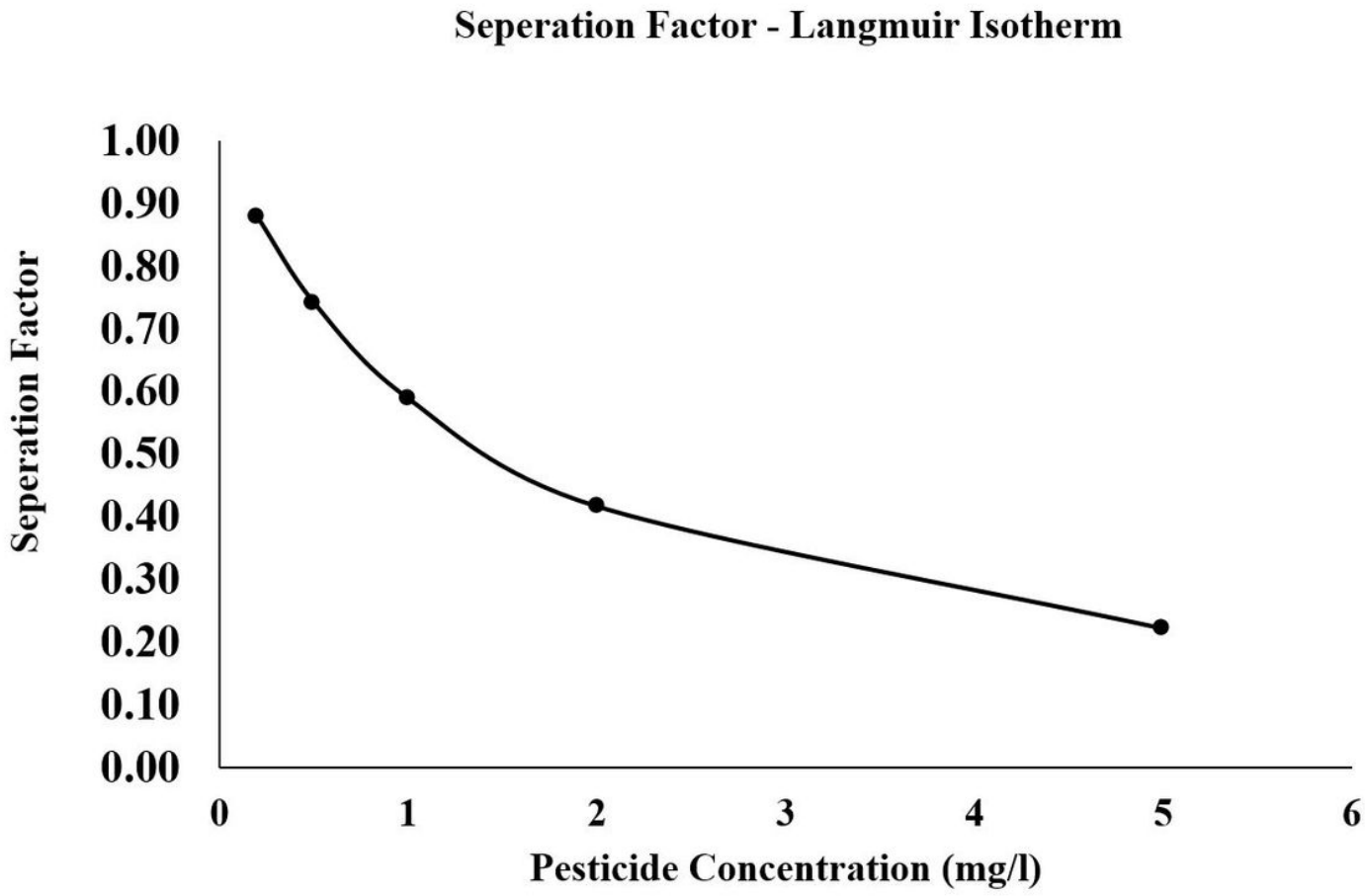

Figure 9

Langmuir Isotherm

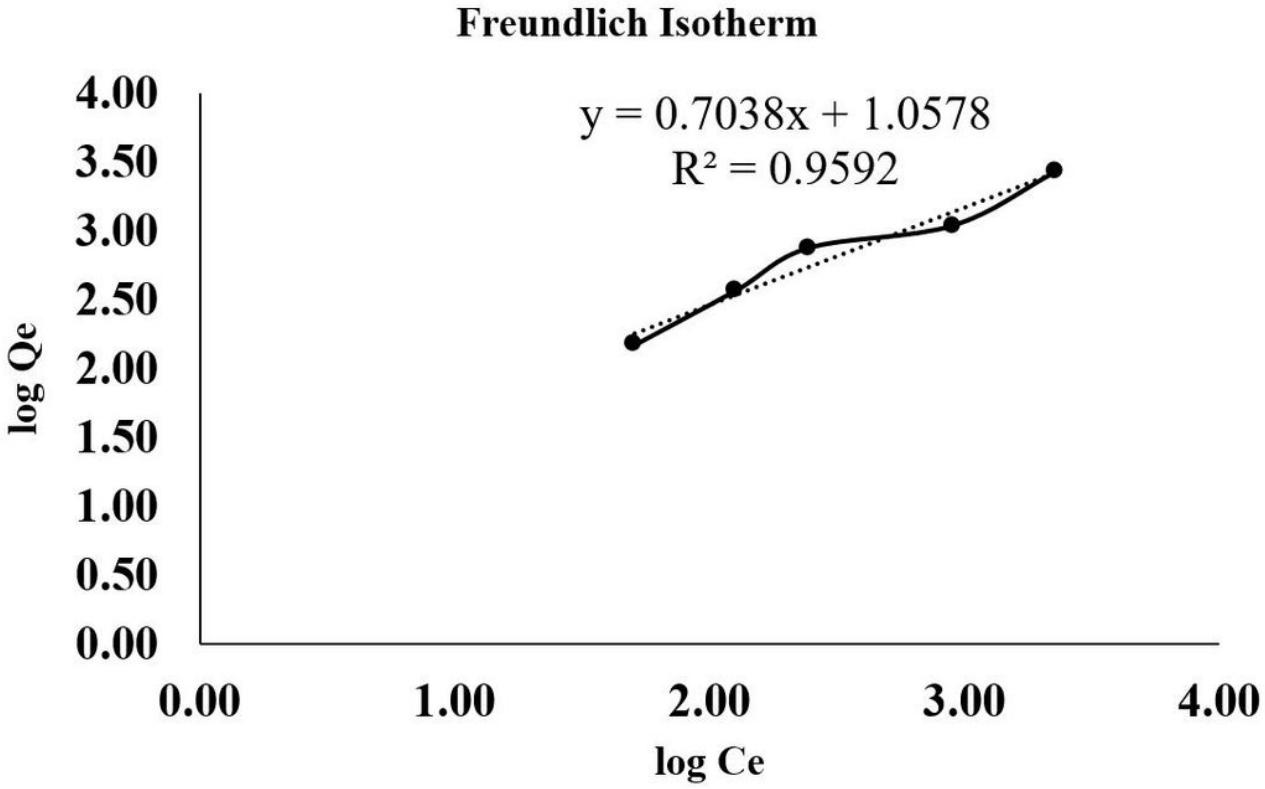

Figure 10

Freundlich Isotherm